Cycling of line-cell phase-change random access memory: Evolution of properties

J.L.M. Oosthoek[1], K. Attenborough[2], G.A.M. Hurkx[2], F.J. Jedema[2], D.J. Gravesteijn[2] and B.J. Kooi[1]
[1] Zernike Institute for Advanced Materials and Materials innovation institute M2i, University of Groningen, Nijenborgh 4, 9747 AG, Groningen, The Netherlands
[2] NXP-TSMC Research Center, Kapeldreef 75, 3001 Leuven, Belgium

ABSTRACT

Doped SbTe phase change (PRAM) line cells produced by e-beam lithography were cycled 100 million times. During cell cycling the evolution of many cell properties were monitored, in particular the crystalline and amorphous resistance, amorphous resistance drift exponent, time dependent threshold voltage, crystallization temperature and activation energy of crystal growth. The power of the present approach is that all these properties were measured simultaneously during the life of single cells. The evolution of the cell properties can be summarized by (i) an initialization phase characterized by settle-in effect of the material surrounding the programmable region, (ii) a usable life phase where initially the cell properties remain fairly constant until after ~$5 \cdot 10^5$ cycles decomposition of the programmed region caused degradation of the cell properties, and (iii) finally an end of life phase where the cell is stuck in the SET state after typically 10^8 cycles. Although generally the threshold voltage is directly related to the amorphous resistance it was found that during cycling this relation is not constant but evolved as well. Instead, the crystallization temperature could be linked to the threshold voltage throughout the complete life cycle of the cell which could lead to new insights to the nature of the threshold event.

Key words: PRAM, line cell, cell cycling, resistance, threshold voltage, resistance drift, decomposition

1. INTRODUCTION

Accurate knowledge and understanding of amorphous resistance drift, threshold voltage, threshold voltage drift and critical properties of non-volatile memories, including data retention (archive stability), program settings (voltages and currents needed to switch between the two or multilevel states of the memory) and cyclability (endurance), are essential for the PRAM technology. Published line cell endurance is currently limited to hundred million cycles.[1,2] Within this limit all the other properties of the memory should ideally be independent of the cycle number. In this work we show detailed results on the evolution of memory cell characteristics during cycling. We measured the resistances, resistance drift, threshold voltage, threshold-voltage drift, crystallization temperature, and activation energy for crystallization during cycling. The uniqueness of the present work is that all these properties have been obtained simultaneously for a single cell with excellent reproducibility when repeating for several cells. Generally the evolution of a single property, like the threshold voltage, with cell cycling is measured.[3] This enables us, to determine more accurately the interdependences of several parameters.

Here, we demonstrate the usefulness of this approach by showing that during cycling the threshold voltage and crystallization temperature of the phase-change material both decrease and follow a remarkable similar evolution. Generally, it is assumed and also demonstrated[3] that the threshold voltage and the amorphous phase resistance are linked in a rigid way. We show that in our measurements the amorphous resistance is not the dominating factor for predicting the threshold voltage. We relate the decrease in threshold voltage and crystallization temperature as cycling progresses to decomposition of the phase-change material. Finally the cell becomes stuck in the (crystalline) SET state after typically 10 to 100 million cycles.

2. EXPERIMENTS

Phase change line cells of dimension 15x75x225nm3 were produced by e-beam lithography. More processing details can be found elsewhere.[4] Wafer pieces containing cells are mounted on a ceramic plate with built-in heating filament

and thermo-couple allowing for a fast and accurate control of the cell temperature. The planar geometry with the low thermal expansion of the ceramic material minimizes the possibility that probe needles run off the bond pads when the temperature is increased. The temperature is controlled with a PID controller and a controllable DC power supply connected to the heating filament. The temperature is kept stable to ±0.1 °C.

The total measurement setup is schematically depicted in Fig. 1d. Contact to the cell was made by a custom built dual probe needle system with a 3.2 kΩ series resistor connected close to the needle. This series resistor limits the SET current after the threshold event and simulates the selection transistor in a memory. A Tektronix AFG3102 arbitrary function generator was used as a pulse generator which can produce any combination (and shape) of SET, RESET and read pulses with pulse edges down to 4 ns. Pulse voltage and currents were monitored by an Agilent DSO6052A digital storage oscilloscope which also provides 50 Ω termination. The cell resistance was measured accurately with a Keithley 2601 source meter. The average of a measurement at 100 mV and -100 mV was taken to reduce the effect of an offset voltage (in the order of 10 mV) present in the system. An RF switch selects between the current channel of the oscilloscope and the source meter (Fig. 1d).

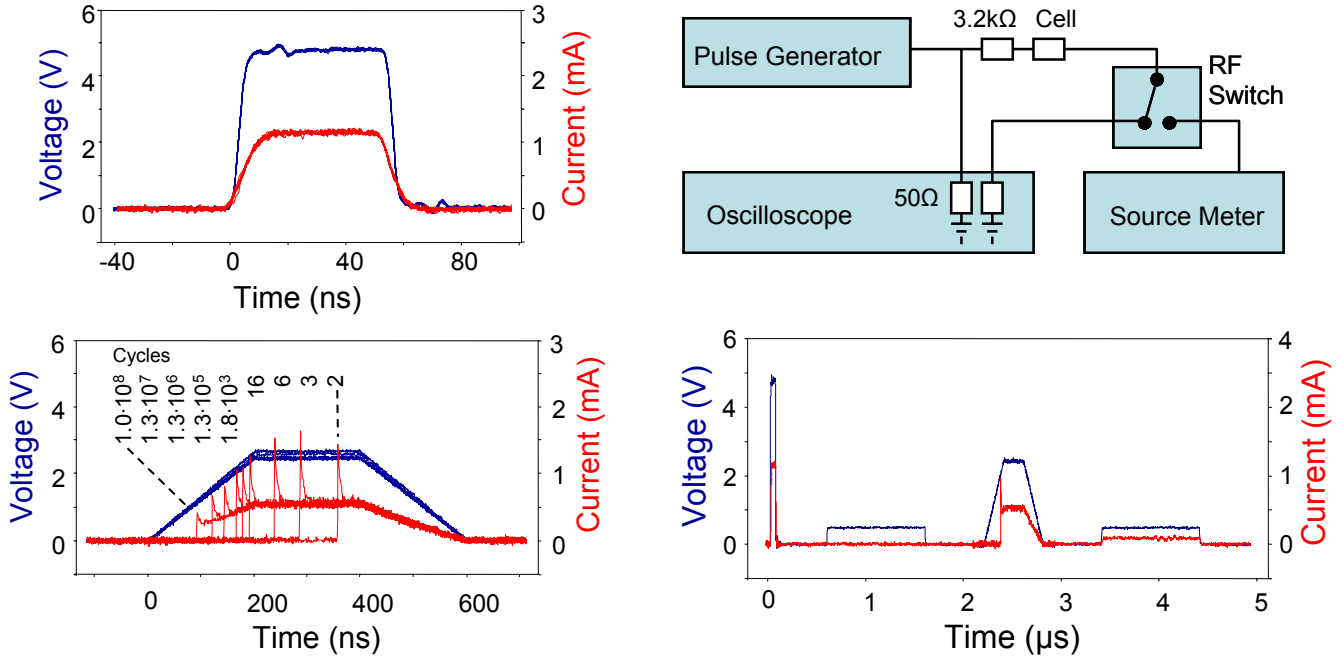

Fig.1 . (a) *Oscilloscope traces of single RESET pulses,* ***(b)*** *single SET pulses and* ***(c)*** *a fast cycle. The latter consists of four separate oscilloscope traces (one for each pulse) from the same measurement. The apparent lower noise of the read pulses arises from averaging performed internally by the oscilloscope when acquiring traces longer than 1000 samples (i.e. traces longer than 250 ns).* ***(d)*** *Setup used for the electrical characterization.*

A complete switching cycle consists either of a single RESET (see Fig. 1a) and SET pulse (see Fig. 1b), where the cell resistance is measured with the source meter after both the RESET and the SET pulse, or a single RESET-read-SET-read pulse sequence (see Fig. 1c), where a complete cycle is performed with a single programmed pulse from the arbitrary function generator which can be repeated up to a million times.

After a single RESET pulse (Fig. 1a) the resistance is measured for 10 seconds as a function of time with exponentially increasing intervals after the RESET event (inset of Fig. 2). It is a well-known fact that the amorphous resistance exhibits a time dependence.[3] It increases (drifts) in time and follows a well-established power law $R_t = R_1 \cdot (t/t_0)^{\alpha}$ where R_1 is the resistance at t_0=1 second after RESET and α is an empirical power law coefficient.[3] From the resistance measurements both R_1 and α were obtained. After the 10 seconds drift the arbitrary function generator is reprogrammed and a single SET pulse (Fig. 1b) crystallizes the cell.

The previous accurate single cycle is only practical for tens or maybe hundreds of cycles as the resistance measurement with the source meter and the switching of the RF relay take considerable time. To cycle the cell millions of times a pulse pattern was programmed into the arbitrary function generator consisting of a RESET – read – SET – read pattern (shown in Fig. 1c). The (1 µs) read pulses validated that the cells were *actually* switched. Ten data

points were collected for each decade of cycling (See Fig. 2 in the results section.). For each of the data points up to ten fast cycles were recorded for validation of switching.

The cycle experiment was periodically interrupted to perform one or more isochronal crystallization measurements. The cell is made amorphous with a single RESET pulse. The resistance is measured for 1000 seconds to allow the cell to drift. The temperature is then increased with a constant ramp rate and the resistance is measured at constant temperature intervals until the cell is crystallized (i.e. when the resistance drops below 10 kΩ). The temperature is returned to 25.0 °C by passive cooling.

The activation energy for crystal growth was obtained from isochronal crystallization measurements with varying ramp rates (ranging from 1 K/minute to 60 K/minute) employing the so-called Kissinger analysis.[5] Between each thermal measurement 10 fast cycles, with identical pulse settings as the general cycling experiment, were performed to bring the cell back to the state after cycling (named hereafter by imprint removal cycle). The imprint removal cycle between the temperature ramps are applied to ensure that the cells were in exactly the same state (R_1, α) for each temperature measurement i.e. to avoid variations in the retention parameters.

3. RESULTS & DISCUSSION

3.1. RESET/SET resistance

The life cycle of the line cells analyzed for the used program settings are shown in Fig.2a, demonstrating that the cells can be switched 10 to 100 million times. The life cycle consists of an initialization phase and a usable life phase until the cell becomes stuck in the SET state (see Fig. 2a).[1,2]

During the initialization phase the amorphous resistance R_1 increases about an order of magnitude from the first to about one hundred cycles. This is accompanied by a measured drop of the drift coefficient α from 0.075±0.007 to 0.04±0.01 during the first 100 cycles (see Fig. 2b). A strong increase of the SET resistance from about 1.3 to 10 kΩ followed by a decrease to about 2 kΩ was observed during the initialization phase (Fig. 2a). These initialization effects can be attributed consistently to stress release and plastic deformation of the material (including soft resist) surrounding the programmable region. A volumetric expansion of the PCM increases R_1 and decreases α.

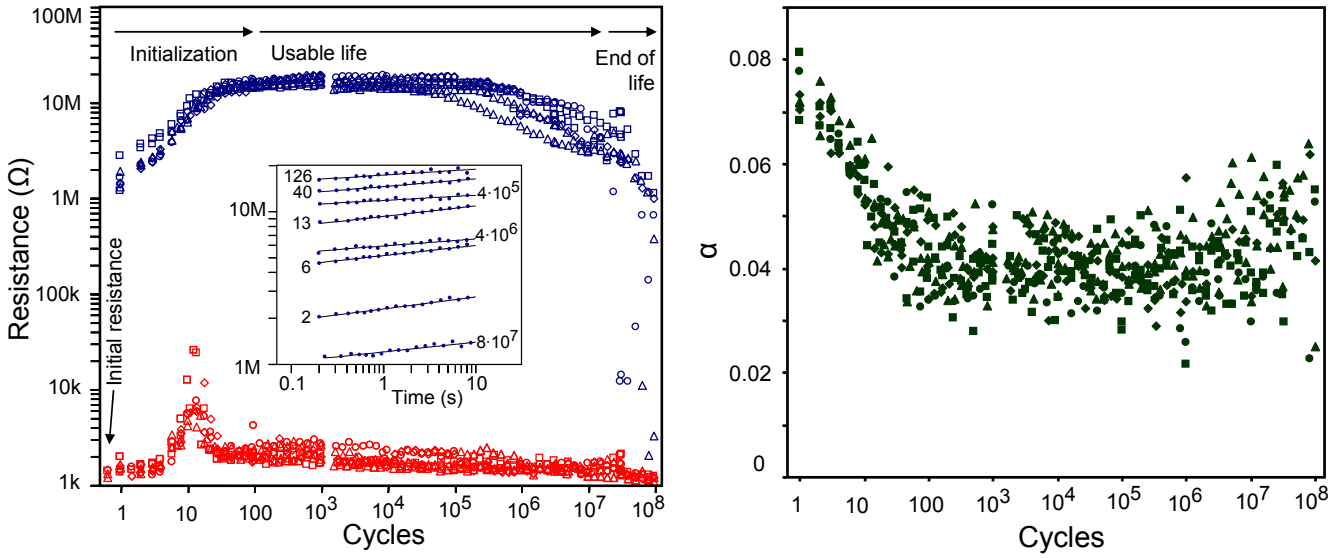

Fig. 2. (a) *A set of complete switching cycles of seven 15x75x225nm3 line-cells. The resistances shown are measured with the source meter after either a single RESET or SET pulse. The amorphous resistance R_1 is always obtained from the time dependent measurement. Inset: A selection of resistance measurements as a function of time (and power law fit) performed at various cycle numbers from which the amorphous resistance R_1 and α were calculated.* ***(b)*** *Drift exponent α measured for the amorphous resistance as a function of the number of switching cycles for the seven cells.*

The usable life phase is characterized by quite stable cell parameters up to about $3.3 \cdot 10^5$ cycles followed by a strong drop in amorphous resistance on a log scale of cycling. Although the amorphous resistance drops significantly the cell can still be switched. Finally the cell can only be brought to the amorphous state by applying a larger magnitude RESET pulse which is recognized here as the end of life phase.

An important observation is that the current during the RESET pulse was not related to the crystalline resistance prior to the pulse. Fig. 1a shows that the oscilloscope traces from the nine RESET pulses, taken at fixed intervals during cycling, overlap considerably. The fact that the pulse voltage traces overlap is trivial but this is not the case for the pulse current traces. Although the crystalline resistance continuously decreases from about 2 to 1 kΩ during the life time, the RESET current was 1.1 mA throughout. This translates to an invariable cell resistance of 1.2 kΩ during melting which was the same for each cell presented in Fig. 2.

3.2. Threshold voltage

The measured threshold voltage as a function of the number of switching cycles is shown in Fig. 3a. Within about 100 cycles the threshold voltage dropped considerably. Fig. 1a shows that during the initialization phase the threshold event occurred during the flat part of the SET pulse shortening the crystallization time. This shorter crystallization time could in fact simply explain the higher SET resistances during this phase as partial crystallization. But successive SET pulses were applied after the threshold event when the SET resistance exceeded 10 kΩ to fully crystallize the cell. However these pulses did not lead to a lower resistance, i.e. did not fully crystallize the amorphous mark.

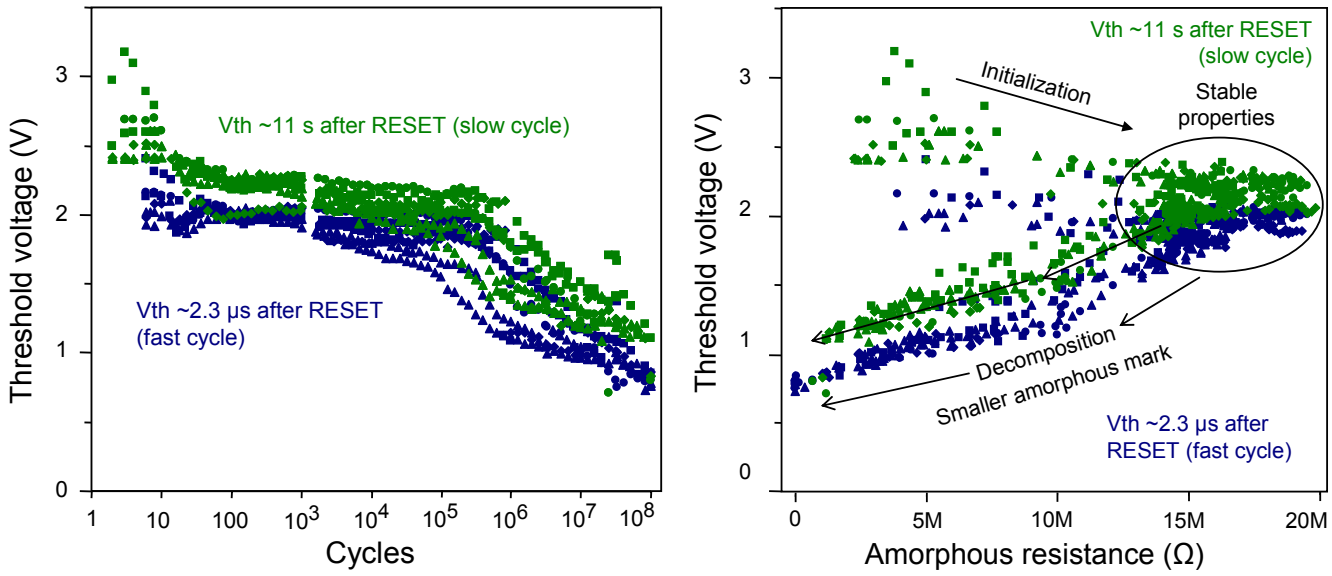

Fig.3. (a) *Threshold voltage as a function of cell cycling measured at 2.3±0.1 µs and ~11 s after RESET.* ***(b)*** *The threshold voltage from the data of Fig. 3a is plotted versus the amorphous-phase resistance from the data of Fig. 2a. For consistency the amorphous resistance at 1.0 s is plotted. However for the slow cycles, the actual resistance during the SET pulse at which the threshold event takes place (~11 seconds after RESET) will be 5 to 22 percent higher depending on the value of α. This difference is very small compared to the evolution of the actual resistance values and does not change the observations. Furthermore, during the fast cycles the resistance cannot be measured that accurately and the amorphous resistance of the slow cycle following that particular fast cycle was used.*

During the usable life phase the threshold voltage is nearly constant up to around 10^5 cycles and then starts to decrease significantly. Fig. 3a also nicely demonstrates that the threshold voltage observed during the SET pulse is dependent on how much time passed after the RESET pulse. The longer the time after the RESET pulse the higher the threshold voltage. This holds for each individual line cell, but does not hold beyond 10^5 cycles when comparing the different cells. This gives Fig. 3a a somewhat chaotic appearance beyond 10^5 cycles. However, also in Fig. 2a it is observed that some cells show a more rapid decrease in amorphous resistance with cycling than others. Therefore it is interesting to correlate the threshold voltage with the amorphous resistance for the (seven) line cells during their life. The result is shown in Fig. 3b. The various phases during the life of the line cells can be readily discerned. In the

initialization phase the amorphous resistance clearly increases and the threshold voltage slightly decreases. During the usable life phase, the threshold voltage and amorphous resistance drop until finally the cell is stuck in the SET state. An interesting observation is that the data are not chaotic beyond 10^5 cycles anymore. For all cells the threshold voltage 2.3 μs and 11 s after the RESET pulse are now well separated. The threshold voltage and amorphous resistance show a dependence that appears to consist of two linear regimes (Fig. 3b). This observation can be explained by two separate processes taking place during the evolution (degradation) of properties induced by cycling.

To gain more understanding on the evolution and behavior of the threshold voltage a more elaborate measurement was performed twice per decade of cycling from 10^3 cycles on. Fig. 4 shows the time dependence of the threshold voltage after the RESET pulse. The threshold voltage was either measured with a single RESET-read-SET-read pulse or by a single RESET and SET pulse with altered delay time. The total time scale spans nine orders of magnitude. Fig. 4 shows that the threshold voltage as a function of time after RESET can be properly fitted with a power law (solid lines) similar to the resistance drift:[3]

$$V_T = V_{T0} + \Delta V_T \left(\frac{t}{t_0} \right)^{\nu} \tag{1a}$$

This power law was proposed by Ielmini et al.[6] and is based on a linear dependence between the threshold voltage and amorphous resistance[3,6]:

$$V_T = V_{T0} + \gamma \cdot R \tag{1b}$$

where γ is a fitting parameter. A natural consequence of Eq. 1b is that the coefficient of resistance drift and threshold drift necessarily must have the same value. Therefore the threshold drift coefficient ν was set equal to the resistance drift coefficient α, obtained from the resistance drift measurements prior to the threshold event, and the parameters V_{T0} and ΔV_T were fitted to the data (also t_0 = 1 s was used). The (left) inset of Fig. 4 shows that both ν and ΔV_T remained fairly constant during cycling: $(41 \pm 2) \cdot 10^{-3}$ and 0.40 ± 0.05 V respectively. However, V_{T0} dropped from 1.7 V to 0.8 V and follows the general evolution of the threshold voltage of Fig. 3a. The biggest drop in ΔV_T occurred between $3.3 \cdot 10^5$ and $3.3 \cdot 10^6$ cycles. As the cell continued to be cycled to $3.3 \cdot 10^7$ the value of ΔV_T continued to decrease until finally at $1.0 \cdot 10^8$ cycles the cell was stuck in the SET state.

Our data can also be fitted with the same degree of accuracy to a linear increase of the threshold voltage on a logarithmic time scale (dashed lines) explained by a theoretical model proposed by Karpov et al.[7]:

$$V_T = V_{T0} \left[1 + \nu \cdot ln\left(\frac{t}{t_0} \right) \right] \tag{2}$$

This model explains the increase of threshold voltage by a random double well potential of a meta-stable disordered atomic structure of a glass. Here the values of V_{T0} and the threshold drift coefficient ν are fitted to the data. The (right) inset in Fig. 4 clearly shows that both V_{T0} and ν evolve during cycling. V_{T0} which is the threshold voltage at t_0 = 1 s, clearly drops significantly which can be expected. However, to keep the slope of the linear fit on log time (fairly) constant ν has to increase by an equal amount. A direct consequence is that according to this model the resistance drift, which remains very constant during cycling, does not follow the evolution of the threshold drift coefficient which doubles.

Furthermore, unlike the amorphous resistance that depends directly on a power law, the threshold voltage dependence in both models has the additive constant V_{T0}. Due to this constant the time dependence of the threshold voltage is numerically weaker than that of the amorphous resistance and both models of Ielmini and Karpov produce very similar results. We expect that a threshold voltage measurement as a function of delay time of at least eleven decades of time are required on cells with high values of α (>0.07) before the validity of either model can be proven on the basis of such a direct measurement. The fit based on the power law (solid line in Fig. 5) is surprisingly similar to the fit based on a linear increase with log time. Therefore no preference between the models can be made on the basis of the accuracy of our data. However, the model of Ielmini (Eq. 1a) predicts the evolution of only V_{T0} while the other fit parameter ΔV_T remains fairly constant. The model of Karpov (Eq. 2) on the other hand implies an evolution of two parameters namely V_{T0} and the threshold drift coefficient ν which we consider to be contradictory to the evolution of the resistance drift.

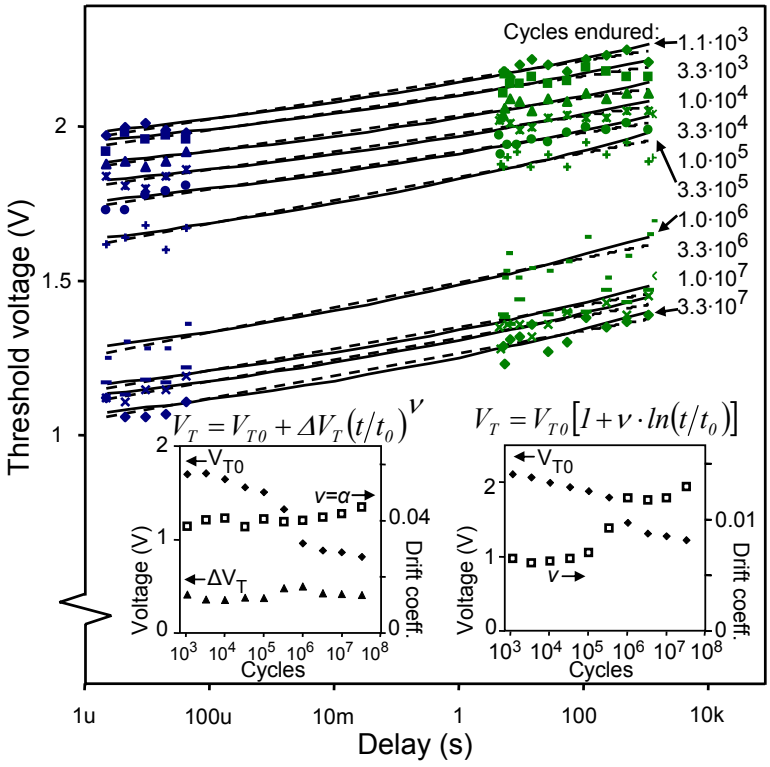

Fig. 4. *The threshold voltage was measured as a function of time after RESET. The measurement was performed twice every decade of cycling from 1.1•10^3 to 3.3•10^7 cycles. The dotted lines are a fit based on a linear increase in log time (model of Karpov et al.)[7], the solid line is a fit based on a power law (model of Ielmini et al.)[6]. The left inset shows the evolution of the fitting parameters based on the model of Ielmini, the right inset shows the evolution of the fitting parameters based on the model of Karpov.*

3.3. Isochronal crystallization

The crystallization temperature was measured at regular intervals during cycling (see Fig. 5). It was found to continuously decrease during cycling from about 125 °C to 90 °C. This continuous decrease is quite unexpected as the amorphous resistance shows stable values at least in the range from 10^2 to 10^5 cycles (Fig. 3a). In this range the crystallization temperature decreases at least 15 °C. Interestingly, the continuous decrease in crystallization temperature is correlated with a continuous decrease in the threshold voltage (Fig. 4).

The crystallization temperature was also measured with ramp rates (φ) of 1, 2, 4, 8, 15, 30 and 60 K/minute (Fig. 6a). The upper inset of Fig. 6a shows the resistance-drift curves prior to the temperature ramp, which overlaps for a time interval of more than three orders of magnitude. This proves that the cell could be returned to an identical state prior to each temperature measurement.

The activation energy of growth was obtained after the various numbers of cycles from Kissinger plots[5] (figures not shown): The slope of $\ln(\varphi/T^2)$ versus T^{-1} gives the activation energy, which was proven for these cells to be the same as the activation energy obtained from isothermal measurements.[2] The activation energy of growth was found to remain within 2.2±0.2 eV during cycling (see Fig. 6b), i.e. no significant evolution with cycling was observed. This is in contrast with the crystallization temperature that shows a relatively dramatic evolution, i.e. decrease with cycling.

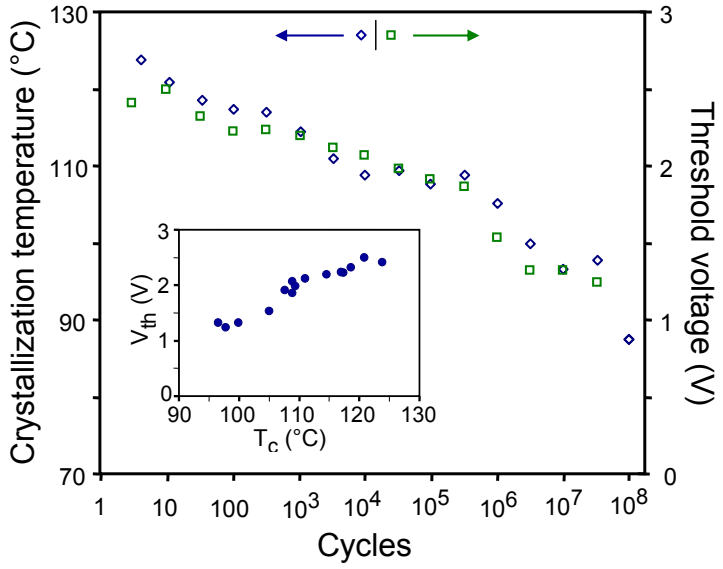

3.4. Coupling evolution of resistances, threshold voltage and crystallization temperature

The conduction mechanism at low carrier concentrations (ohmic region at low read voltages) is fundamentally different from the conduction mechanism at high carrier concentrations. The

Fig. 5. *The threshold voltage and the crystallization temperature at a ramp rate of 30 K/min versus the number of switching cycles. The crystallization temperature was measured the cycle directly following the threshold voltage. Both the threshold voltage and the crystallization temperature show a strong correlation during cycling (see inset).*

RESET (and also SET) pulse always leads to a large current density (typically $7 \cdot 10^{11}$ A/m^2 during the RESET pulse) and large electric fields (~10^7 V/m) within the line cell. During the RESET pulse (and SET pulse), the atoms in the programmed region become mobile.[8,9] Atoms can be ionized and Sb^{3+} and Te^{2-} will move in opposite directions to the electric field. This movement particularly occurs in the molten region during the RESET pulse.[9]

A natural consequence of this ionization of mobile atoms is that electro-migration will take place during cycling and that the phase-change material will experience decomposition. Our observations show that the end of the usable life phase of the line cell is characterized by a decrease of (i) the amorphous resistance (see Fig. 2a), (ii) crystalline resistance (see Fig. 2a), (iii) threshold voltage (see Figs. 3 and 4) and (iv) crystallization temperature (see Fig. 5). These observations are indeed consistently explained by decomposition of the programmed region caused by electro-migration. During the RESET pulses the ionized atoms move in different directions with respect to the electric field. This will lead to regions enriched in either Sb or Te. Starting from the homogeneous phase-change alloy the decomposed alloy will always lead to a lowering of the crystallization temperature. It will be more difficult to produce amorphous regions in the decomposed material since a part of the melt-quenched region is able to re-crystallize. Therefore, with smaller amorphous marks the amorphous resistance and threshold voltage will decrease.[10]

Our measurements clearly indicate that the molten region during the RESET pulse is not affected by cycling; only quenching of this molten state into the amorphous state becomes increasingly difficult beyond ~$3.3 \cdot 10^5$ cycles. Finally amorphous marks cannot be produced (with the standard pulse settings) anymore beyond 10^7 or 10^8 cycles and the cell becomes stuck in the SET state (end of life). This is exactly what we observe and is thus consistently explained by electro-migration induced decomposition of the phase-change material. Only with increasing the magnitude of the RESET pulse an amorphous region can be created. The region that melts during the pulse needs to be much larger to accommodate re-crystallization. However, then also decomposition is accelerated by the higher programming current.

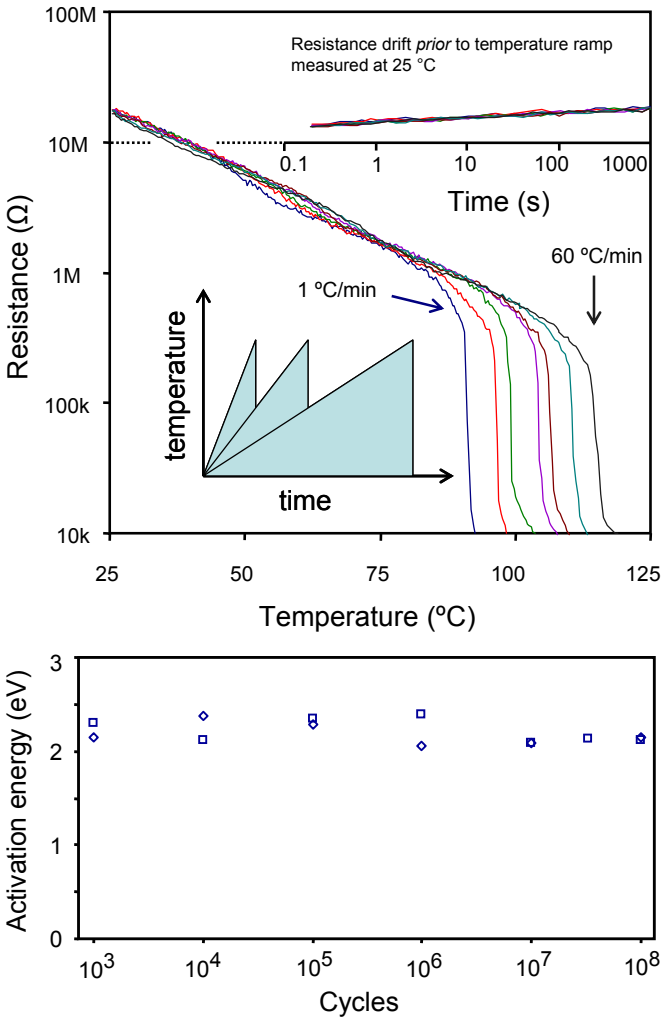

Fig. 5 shows that during cycling the crystallization temperature (measured at a ramp rate of 30 K/minute) decreased continuously from 125°C to 90°C. This decrease in crystallization temperature is accompanied by a decrease in threshold voltage. Although a reduction in programmed volume (length of the amorphous mark) will lead to a lower crystallization temperature and threshold voltage, it cannot, on its own, explain the drop in both quantities over the complete life of the cells. However, it can be associated with part of the life cycle, in particular after $3.3 \cdot 10^5$ where re-crystallization of the amorphous region is believed to become apparent. Our conclusion is that the threshold voltage and crystallization temperature are both closely related to the decomposition of the amorphous volume (see inset of Fig. 5). The decomposed material, with separate regions

Fig. 6 (a) *A cell was switched to the RESET state and drifted for 1000 s while the resistance was measured (upper inset). Immediately after the drift period the temperature was raised with a constant ramp rate until the cell crystallized. This was repeated for various ramp rates as schematically depicted in the lower inset.*
(b) *The activation energy for crystallization (E_C) versus the number of switching cycles. E_C was obtained from the crystallization temperature measured at different ramp rates using the Kissinger analysis. Unlike the crystallization temperature at a fixed ramp rate the activation energy does not show a significant evolution during cycling.*

enriched in either Sb or Te, exhibits an overall lower crystallization temperature. As a consequence the amorphous-phase resistance and the threshold voltage also decrease. The threshold field, at which electrical breakdown occurs, is known to vary greatly among materials.[1,11] Furthermore, the extrapolated threshold voltage at zero amorphous mark size is finite and also material dependent.[6,11,12] The phenomenological threshold voltage is therefore related to both quantities and the length of the amorphous mark. A decrease of both the crystallization temperature and threshold voltage accompanied by a decrease of the amorphous resistivity of almost an order of magnitude was observed for increasing the Sb content in Sb_xTe_{1-x} alloys ($x \geq 0.64$)[10] which is consistent with our data.

4. CONCLUSIONS

This work presents an extensive study on phase change random access memory, and in particular the horizontal line cell geometry.[1] Many cell properties (i.e. the amorphous and crystalline resistances, amorphous resistance drift, threshold voltage, threshold-voltage drift, crystallization temperature, and activation energy for crystallization) were measured during cell cycling on the same cells and can therefore be directly related. Cells can typically be cycled 100 million times and show stable properties after an initialization phase of about 100 cycles up to about $5 \cdot 10^5$ cycles. Beyond this number of cycles the amorphous resistance, the threshold voltage and the crystallization temperature decrease significantly. This behavior is attributed to electromigration induced decomposition of the active phase-change material in the line cell.

Generally, it is assumed and also demonstrated that the threshold voltage (V_T) and the amorphous phase resistance (R_a) are linked in a rigid way. We show that in our measurements the R_a is not the dominating factor for predicting the threshold voltage V_T. By varying the magnitude of the RESET pulse the R_a shows a peak value while the threshold voltage V_T continuously increases leading to both a positive and negative dependence between R_a and V_T. Furthermore, the evolution of the threshold voltage can be linked to the evolution of the crystallization temperature. The crystallization temperature and threshold voltage appear to continuously decrease during cycling due to electromigration induced decomposition and follow a remarkably similar trend.

As the crystallization temperature drops, the molten region can partly re-crystallize as it is melt-quenched, *i.e.* more time is spent above the crystallization temperature leading to smaller amorphous mark, which starts to become apparent beyond $\sim 3.3 \cdot 10^5$ cycles. Finally the cell becomes stuck in the SET state after typically 10 to 100 million cycles. Although the material is still molten during the application of a RESET pulse this does not load to an amorphous melt-quenched state as the cell fully crystallizes directly after the pulse.

REFERENCES

1. M.H.R. Lankhorst, B. Ketelaars, and R.A.M. Wolters, Nature Materials **4,** 347 (2005).
2. J.L.M. Oosthoek, B.J. Kooi, K. Attenborough, G.A.M. Hurkx, D.J. Gravesteijn, Mater. Res. Soc. Symp. Proc. Vol. 1250, G14-04 / H07-04 (2010).
3. A. Pirovano, A.L. Lacaita, F. Pellizzer, S.A. Kostylev, A. Benvenuti, and R. Bez, IEEE Transactions on Electron Devices **51,** 714 (2004).
4. F.J. Jedema, M.A.A. in 't Zandt, and W.S.M.M. Ketelaars, Appl. Phys. Lett. **91,** 203509 (2007).
5. H. E. Kissinger, Analytical Chemistry **29**, 1702 (1957).
6. D. Ielmini, A.L. Lacaita, and D. Mantegazza, IEEE Transactions on Electron Devices **54,** 308 (2007).
7. I.V. Karpov, M. Mitra, D. Kau, G. Spadini, Y.A. Kryukov, and V.G. Karpov, J. Appl. Phys. **102,** 124503 (2007).
8. D.M. Kang, D. Lee, H.M. Kim, S.W. Nam, M.H. Kwon, and K.B. Kim, Appl. Phys. Lett. **95**, 011904 (2009); ibid. **94**, 193504 (2009); ibid., Electrochem. Sol. State Lett. **12**, H155 (2009).
9. Tae-Youl Yang, Il-Mok Park, Byoung-Joon Kim, Young-Chang Joo, Appl. Phys. Lett. **95**, 032104 (2009).
10. M.S. Youm, Y.T. Kim, Y.H. Kim, and M.Y. Sung, Physica Status Solidi (a) **205**, 1636 (2008).
11. D. Krebs, S. Raoux, C. T. Rettner, G. W. Burr, M. Salinga, and M. Wuttig, Appl. Phys. Lett. **95,** 082101 (2009)
12. V.G. Karpov, Y.A. Kryukov, S.D. Savransky, and I.V. Karpov, Appl. Phys. Lett. **90,** 123504 (2007).

Biography Prof. dr. ir. B.J. Kooi

Head of the research group "Nanostructured Materials and Interfaces", Zernike Institute for Advanced Materials, University of Groningen, The Netherlands.

Research focus of the group: structure-property relations for nanostructured materials or interfaces/surfaces with main current topics on phase-change materials, ferroelectric thin films, nano-clusters, micro- and nano-resonators and surface forces. Main experimental facilities include Transmission Electron Microscopy, Scanning Probe Microscopy and a dedicated nano-cluster deposition system.

Jan. 1991 - Jan. 1995: Ph.D. student in the section 'Physical Chemistry of the Solid State' under supervision of prof. dr. ir. E.J. Mittemeijer, Laboratory for Materials Science, Delft University of Technology.

Publications: Over 150 publications in international peer-reviewed scientific journals and proceedings.